

Remote sensing to assess the risk for cultural heritage: forecasting potential collapses due to rainfall in historic fortifications

Mónica Moreno, Rocío Ortiz and Pilar Ortiz
*Departamento de Sistemas Físicos, Químicos y Naturales,
Pablo de Olavide University, Sevilla, Spain*

Abstract

Purpose – Heavy rainfall is one of the main causes of the degradation of historic rammed Earth architecture. For this reason, ensuring the conservation thereof entails understanding the factors involved in these risk situations. The purpose of this study is to research three past events in which rainfall caused damage and collapse to historic rammed Earth fortifications in Andalusia in order to analyse whether it is possible to prevent similar situations from occurring in the future.

Design/methodology/approach – The three case studies analysed are located in the south of Spain and occurred between 2017 and 2021. The hazard presented by rainfall within this context has been obtained from Art-Risk 3.0 (Registration No. 201999906530090). The vulnerability of the structures has been assessed with the Art-Risk 1 model. To characterise the strength, duration, and intensity of precipitation events, a workflow for the statistical use of GPM and GSMap satellite resources has been designed, validated, and tested. The strength of the winds has been evaluated from data from ground-based weather stations.

Findings – GSMap precipitation data is very similar to data from ground-based weather stations. Regarding the three risk events analysed, although they occurred in areas with a torrential rainfall hazard, the damage was caused by non-intense rainfall that did not exceed 5 mm/hour. The continuation of the rainfall for several days and the poor state of conservation of the walls seem to be the factors that triggered the collapses that fundamentally affected the restoration mortars.

Originality/value – A workflow applied to vulnerability and hazard analysis is presented, which validates the large-scale use of satellite images for past and present monitoring of heritage structure risk situations due to rain.

Keywords Remote sensing, Risk, Vulnerability, High precipitation, Rammed Earth, Historic fortification, Art-risk, Collapse

Paper type Research paper

© Mónica Moreno, Rocío Ortiz and Pilar Ortiz. Published by Emerald Publishing Limited. This article is published under the Creative Commons Attribution (CC BY 4.0) licence. Anyone may reproduce, distribute, translate and create derivative works of this article (for both commercial and non-commercial purposes), subject to full attribution to the original publication and authors. The full terms of this licence may be seen at <http://creativecommons.org/licences/by/4.0/legalcode>

This study has been based on the methodology developed by the 4 projects: 1) Art-Risk (BIA2015-64878-R) RETOS project of Ministerio de Economía y Competitividad and Fondo Europeo de Desarrollo Regional (FEDER), 2) FENIX (PID2019-107257RB-I00) financed by MCIN/AEI/10.13039/501100011033/FEDER “A way to build Europe”, 3) RESILIENT-TOURISM (PYC20 RE034 UPO) project of Consejería de Transformación Económica, Industria, Conocimiento y Universidades, Junta de Andalucía, 4) MURALLAS, Diagnosis and Cataloging of Andalusian Architectural Heritage through Risk and Vulnerability Analysis (UPO 20.01) project of Consejería de foment, infraestructura y ordenación del territorio, Junta de Andalucía; and the research teams TEP-199 (Patrimonio, Medioambiente y Tecnología) and Sanit-ARTE laboratory. M. Moreno is grateful to the State Program for the Promotion of Talent and its Employability in R+D+i of the Ministry of Science and Innovation of Spain for his technical fellowship, PTA2019-016882 funded by MCIN/AEI/10.13039/501100011033. Funding for open access publishing: Universidad Pablo de Olavide.



1. Introducción

Torrential rainfall is one of the primary weather hazards in Europe and can act as triggers for floods, landslides and damage to infrastructure and buildings (Schauwecker *et al.*, 2019). In the coming years, climate change is expected to modify precipitation patterns on a global scale, increasing the risk levels associated with heavy precipitation events (Hosseinzadehtalaei *et al.*, 2020; Kharin *et al.*, 2013; Tabari, 2020; Trenberth, 2011). The strong winds during the storm cause the water to fall obliquely and forcefully splash the wall (Luo *et al.*, 2019). In continental climates with strong winds, the studies carried out by Su *et al.* (2022) have identified erosion processes up to 10 times stronger in rammed Earth walls located in the windward. In the scenario described, heritage structures constructed with Earth are particularly vulnerable (Beckett *et al.*, 2020; Bonazza *et al.*, 2021; Cacciotti *et al.*, 2021). This is the case for medieval rammed Earth fortifications, in which the infiltration of water into the interior of the walls causes erosion, loss of material (Beckett *et al.*, 2020) and, in the worst-case scenarios, collapse (Drdácký and Cacciotti, 2020). Faced with this type of problem, monitoring, preventive conservation, and restoration work becomes an essential activity to reduce the vulnerability of structures and to prevent damage during the rainy season.

In the long term, minimising the risk of loss of cultural elements requires articulated decision-making and management strategies. From this theoretical framework, different methodological proposals have emerged that analyse dangerous scenarios in heritage contexts using Risk Index and Geographic Information Systems (GIS) (Bonazza *et al.*, 2021; Ferreira and Santos, 2020; Figueiredo *et al.*, 2021; Sabbioni *et al.*, 2010; Sesana *et al.*, 2020; Canivell *et al.*, 2020; Gutiérrez-Carrillo *et al.*, 2020). Within these proposals, the Art-Risk model, which have received the Europa Nostra 2021 award for heritage conservation research, include multilevel systems that are based on very simple work tools to collect data *in situ*, and then overlay increasingly complete and complex proposals for the analysis of vulnerability, hazards and risks (Cagigas-Muñiz *et al.*, 2018; Ortiz *et al.*, 2018; Prieto *et al.*, 2020).

The Art-Risk 3.0 software (Moreno *et al.*, 2022a; Cagigas-Muñiz *et al.*, 2020) is designed to analyse groups of heritage buildings and assess which ones are at higher risk of loss. Applied to the monitoring of rainfall hazards, the Art-Risk 3.0 tool has a GIS (Moreno *et al.*, 2022b) that, by entering the coordinates of a heritage asset located in Spain, indicates the hazard values according to average precipitation, its intensity and the probability of flooding from the climate data from the last 30 years (Ortiz Calderon *et al.*, 2021). The Art-Risk 1 model is based on a Leopold matrix adapted to record vulnerability according to conservation status. Used together with the Art-Risk 3.0 software allows to describe risk scenarios in detail (Moreno *et al.*, 2019; Ortiz and Ortiz, 2016).

In order to advance in the design of models that enable the prediction of risk situations, it is necessary to assess historical data and past occurrences. For this, the Art-Risk model use workflows developed for monitoring changes in climatic hazards through the use of historical series of satellite images (Moreno *et al.*, 2021, 2022c).

From this perspective, this research proposes an analysis of three rainfall emergencies that caused damage to medieval fortifications located in southern Spain between 2017 and 2021. The main objective is to identify the characteristics of force, intensity and duration of the rainfall that triggered the emergency, the degree of vulnerability presented by the damaged structures and the climatic hazard of the environment through the use of satellite resources. For this, the use of the different hierarchical modules of the Art-Risk methodology is proposed. The Art-Risk 3.0 module (Moreno *et al.*, 2022b) quickly categorises the climatic hazard due to rainfall into the three contexts analysed. The second, more complex module describes the risk scenario through the use of Art-Risk 1 vulnerability matrices (Moreno *et al.*, 2019; Ortiz Calderon *et al.*, 2021) and satellite images from the Global Precipitation Measurement (GPM) and Global Satellite Mapping of Precipitation (GSMaP) missions.

This study presents and tests, a workflow capable of monitoring the volume of rainfall and the duration in hours of a past rainfall emergency that cause damage in rammed Earth fortifications. As far as the authors have searched, no similar references have been found.

The results obtained allow to evaluate the reliability offered by GPM and GSMaP for real-time monitoring, better understand the specific circumstances that caused the emergency situations under analysis, and forecast future weather hazards that may cause damage to earthen heritage structures. In turn, this method can be combined with the methodology previously designed for the identification of climatic extreme precipitation events through the use of CHIRPS and PERSIANN satellite resources (Monica *et al.*, 2022c).

2. Material and methodology

2.1 Case studies

The study area is southern Spain and the three rainfall emergencies analysed are those that occurred in the fortifications of Marchena in 2017, Niebla in 2019 and Almería in 2021 (Figure 1).

Niebla is located on a Huelva plain on the banks of the Tinto River. It currently preserves a large part of the medieval rampart (Figure 2a). The origin of the defensive system is pre-Roman (8th-7th centuries BC), but the preserved remains correspond to the Islamic reforms and extensions of the Almohad period (12th century) (Canivell and González, 2013). The rampart is built of monolithic rammed Earth improved with lime. On 21 December 2019, heavy rainfall caused collapses in several of its sections (ABCandalucía, 2020).

Marchena is located on the plain of the Sevillian countryside. It preserves fortified remains of the rampart, the citadel and a recreational area associated with the citadel (Figure 2b). The fortified remains are from the Almohad Islamic period (13th century) (Valor Piechotta, 2004) and are constructed in a monolithic rammed Earth improved with lime. In November 2017, heavy rainfall caused the collapse of one of the towers belonging to the city wall (ABCdesevilla, 2017).

Almería is a coastal city in south-eastern Spain. It preserves a large portion of the citadel, and some sections of the city wall from the Islamic Caliphate period (10th - 11th centuries) with extensions from the Taifa period (11th century) (Gurriarán, 2020; Luque, 2014) (Figure 2c). The Alcazaba (citadel) is made of a monolithic rammed earthen improved with lime. Despite the fact that Almería has a sub-desert climate, in November 2021 the rainfall caused erosion and landslides at one of the *Arrabal* district towers (Diario de Almería, 2021).

2.2 Satellite resources used

Precipitation data has been obtained from the *Global Satellite Mapping of Precipitation* (GSMaP) reanalysis produced from the *Global Precipitation Measurement* (GPM) satellite constellation, an international network with the GPM Core as its main satellite. GPM has sensors for precipitation measurement that operate within the visible/infrared (IR) and microwave (PMW) ranges (Bolvin *et al.*, 2015; Huffman *et al.*, 2020).

IR sensors are carried by satellites located in geostationary orbits (GEO) located 36,000 km above the Earth and cover large areas with very high temporal resolution. These sensors use the correlation between cloud top brightness temperature and rainfall development as an indirect indicator of rainfall occurrence. Although this type of sensor confuses cirrus clouds with the presence of rainfall and does not detect precipitation that

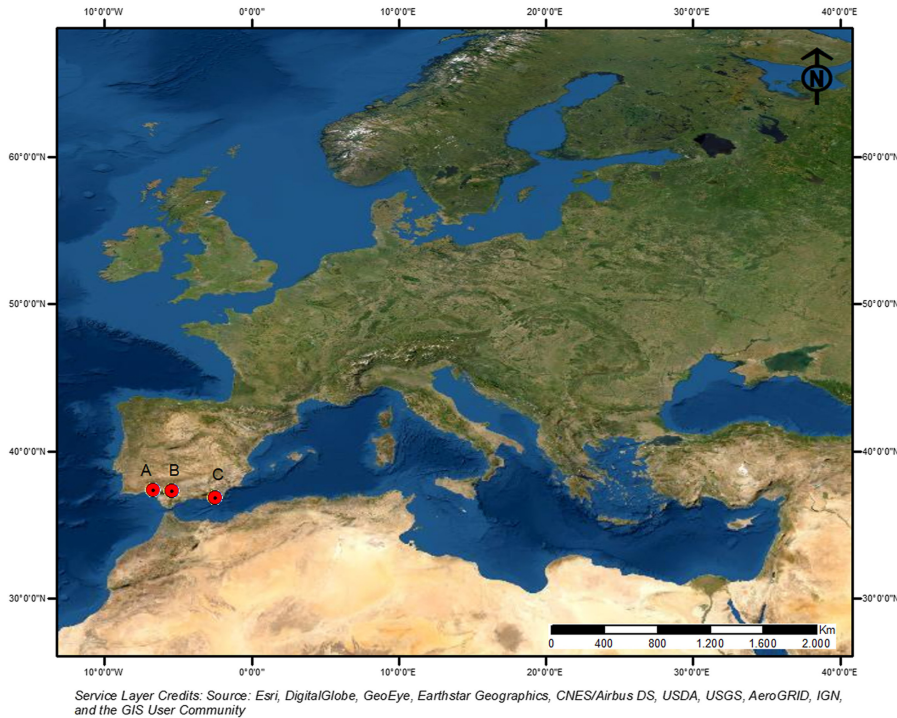


Figure 1.
Study area: (a) Niebla;
(b) Marchena; y (c)
Almería

occurs at low altitudes (Liang, 2017; Sun *et al.*, 2018) they are used because they offer high temporal resolution.

PMW sensors measure the natural release of water droplets within this range of the light spectrum. They are direct measurements that offer more reliable data than those obtained via IR. Despite their location on Low Earth Orbit (LEO) platforms, which implies low temporal resolution (Liang, 2017; Sun *et al.*, 2018) they are used because they offer very reliable data.

The GPM mission, led by the National Aeronautics and Space Administration (NASA), enables the combination of data obtained by a constellation of IR and PMW sensors using the IMERG algorithm (Huffman *et al.*, 2020). Thus, the satellite images offered by GPM-IMERG combine the improvements of both sensors: they increase the temporal resolution of PMW data and minimise the uncertainty associated with IR data (Huffman *et al.*, 2020). The available satellite images provide the precipitation rate (mm/30 min) with a spatial resolution of 0.1° (approx. 11 km) from the year 2000 to the present. The available bands include the values collected individually by the IR and PMW sensors, as well as and the combination thereof through IMERG.

In turn, the GSMaP reanalysis belonging to the Japanese Space Agency (JAXA) provides an adjustment of the GPM satellite data to the values of ground-based weather stations (Mega *et al.*, 2019; Okamoto *et al.*, 2005). The resulting images show the precipitation rate (mm/hr) with a spatial resolution of 0.1° (approx. 11 km) from the year 2000 to the present.

In order to know the reliability of the output data for each satellite resource, this study compares the values shown by the GPM IR and PWM sensors, the combined values of the

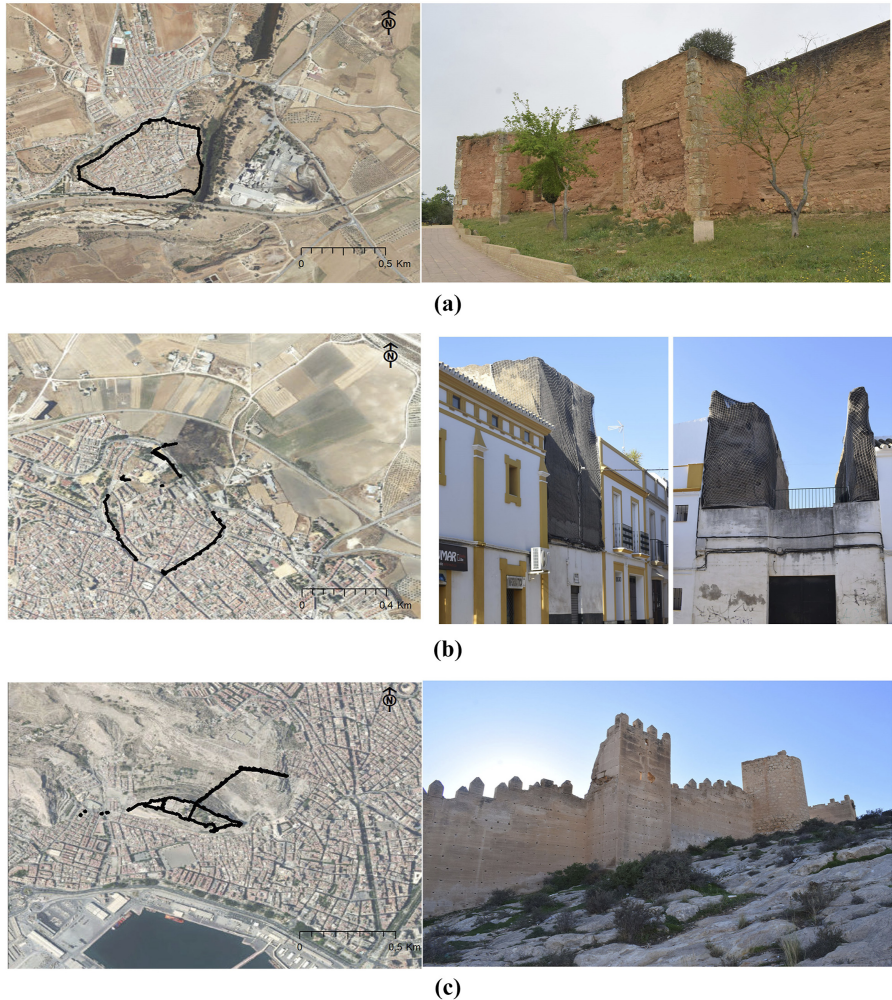


Figure 2. Ortophotograph with the preserved medieval fortifications highlighted in black and current detail view of the sections affected by the rainfall: (a) Niebla; (b) Marchena; y (c) Almería

IMERG algorithm and the values adjusted to GSMaP ground-based stations with the ground-based weather stations of the Spanish Meteorological Agency (AEMET).

2.3 Workflow

The past rainfall emergencies were selected from a bibliographic search in the press (ABCandalucía, 2020; ABCdesevilla, 2017; Diario de Almería, 2021).

The climatic hazard from the environment surrounding Niebla, Marchena and Almería was evaluated using the Art-Risk 3.0 tool (Moreno *et al.*, 2022a, b, c; Cagigas-Muñoz *et al.*, 2020). For the Spanish territory, this tool allows coordinates to be entered and the hazards from the environment to be obtained according to a hazard scale from 1–5. Of the 7 variables provided by Art-Risk 3.0, this study has only used the 3 variables related to rainfall hazard: average rainfall, rainfall erosivity and probability of flooding. Table 1 shows the qualitative assessment used by

the GIS of Art-Risk 3.0 to classify the output hazard values. The average precipitation indicates the climatic average of the volume of annual precipitation per surface unit (mm/m²) over the last 30 years. The rainfall intensity coefficient indicates the relationship between hourly rainfall and the corrected daily average. The data on flood zones corresponds to that defined by the National Flood Zone Mapping System based on different return periods (Moreno *et al.*, 2022a, b, c). Art-Risk 3.0 is available at: <https://www.upo.es/investiga/art-risk-service/art-risk3/> and has manuals to interpret the results obtained (Ortiz *et al.*, 2019).

The vulnerability of the 3 fortifications was evaluated at the wall level using the assessment matrix and the vulnerability index for rammed Earth walls from the Art-Risk 1 model (Moreno *et al.*, 2019). For this reason, the 3 fortifications located in public spaces were divided into minimum analysis units (tower and walls) Marchena was divided into 40 minimum analysis units, Niebla into 106 and Almería into 101. This matrix includes a list of rammed Earth wall weathering forms and their magnitude or capacity to cause damage (Table 2). The frequency of the weathering forms in each wall was recorded manually with values of 1–3 (1: low, 2: medium and 3: high) and the intensity of the damage was obtained from the following equation $I_i = M_i + (F_i - 1)$ where I is the intensity, M is the magnitude and F is the frequency (Ortiz and Ortiz, 2016).

The vulnerability index (VI) was obtained by dividing the total value of the alteration indicator intensities recorded for each wall (V_x) by the sum of the total value of the alteration indicator intensities ($\sum vdp$) if their presence was 3 (most unfavourable situation) (Ortiz and Ortiz, 2016).

$$VI = V_x / \left(\sum_{f=3} vdp \right) \times 100$$

Once the vulnerability index was calculated, the results were migrated to a GIS according to the methodology developed by (Moreno *et al.*, 2019) and grouped into 5 vulnerability groups in accordance with a classification of natural breaks based on the Jenks algorithm to maximise the

Categories	GIS variable	Qualitative valuation
Environmental hazards by precipitation	Average Rainfall (AR16)	(1) very low: <600 mm/m ² ; (2) low: 600–700 mm/m ² ; (3) moderate: 750–1,000 mm/m ² ; (4) high: 1,000–1,200 mm/m ² ; (5) very high: >1,200 mm/m ²
	Raindrop impact: rain intensity coefficient (AR17)	(1) very low: <7; (2) low: 7–8; (3) moderate: 8–9; (4) high: 9–10; (5) very high: >10
	Flooding hazard (AR21)	(1) very low: not floodable; (2) low: return period 500 years; (3) moderate: return period 100 years; (4) high: return period 50 years; (5) very high: return period 10 years

Table 1.
Rainfall hazard variables applied from the art-risk 3.0 model

Weathering form group	Weathering forms and magnitude
Discoloration and deposits	Moist area (5); efflorescence (3); concretion (3); pigeon droppings (2); surface deposit (1); coloration or discoloration (1); iron rich patina (1); soiling (1)
Fracture and deformations	Fragmentation (10); fracture (5); deformation (3); crack (2)
Losses of material and detachment	Detachment (5); missing part (5); erosion (4); alveolization and cavernization (4); differential alteration (4); sanding (4); scaling (3); scratching (1)
Biological colonization	Vegetation (3); biological colonization (2)

Table 2.
Magnitude of the weathering forms according to the art-risk 1 model

differences between classes. This statistical classification tool is available in most of the Geographic Information System softwares. The natural breaks method partitions classes based on the natural and inherent groupings of the data. The results obtained reduce the variance within a group of data and maximize the variance between the other groups (Smith, 2018).

The characteristics of the rainfall that caused the emergency situations were assessed from the GPM and GSMaP satellite resources in the Google Earth Engine (GEE) satellite analysis software. As far as the authors have searched, no similar references have been found in Heritage studies of this type.

In order to observe the behaviour of the estimated precipitation models of the GPM-IR, GPM-PMW, the GPM-IMERG combination and the GSMaP adjustment, daily precipitation data from over three months of the rainy season (January–March 2021) was obtained in the GEE and was compared with the data obtained by the ground-based stations of the Spanish Meteorological Agency (AEMET). AEMET data has been selected as the quality standard because it is taken according to the recommendations of the World Meteorological Organisation ([Organización Meteorológica Mundial, 2012](#)). For each of the GPM satellite resources (IR, PMW and IMERG), which provides data every 30 min, 4,320 images were analysed and 2,160 images for GSMaP, which provides data every hour. The GSMaP coefficient of determination with respect to the AEMET values was calculated to quantify the adjustment provided in the three study areas analysed. The points analysed correspond to the coordinates of the AEMET stations closest to the three collapse cases analysed: Almería airport (36.846389; -2.356942), Morón de la Frontera (37.164459; -5.611393) and Huelva (37.278359; -6.911664).

The precipitation values collected by GSMaP for the coordinates and dates on which the damage occurred were used to analyse the precipitation events that occurred in Niebla, Marchena and Almería. Subsequently, information was collected regarding the strength, duration and intensity of the rainfall from satellite images.

The strength of the precipitation was defined as a function of the volume of daily rainfall (mm/day). This variable was categorised according to the Alpert classification (2002) for the Spanish Mediterranean area, which distinguishes light rainfall (<4 mm/day); light-moderate (4–16 mm/day); moderate-strong (16–32 mm/day); strong (32–64 mm/day); strong-torrential (64–128 mm/day); and torrential (>128 mm/day).

The duration was established according to the number of hours that the rain lasted and the intensity according to the distribution of the volume of rain that fell during the period of time that the event lasted. In order to assess the hazard by its intensity, the scale defined by the AEMET was used, which establishes 15 mm/hour as the minimum threshold for rainfall to be considered heavy with the associated risk (AEMET, 2015).

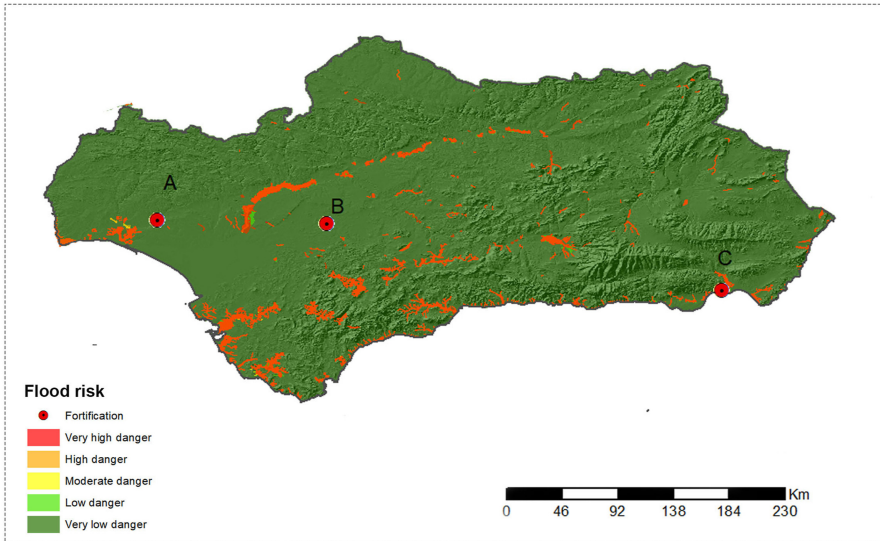
The direction, average daily speed and wind gusts (maximum speeds per hour) were obtained from data from AEMET weather stations. The threshold for a wind to be considered strong was 40 km/h (AEMET, 2015).

3. Results and discussion

3.1 Climatic hazard from local rainfall patterns

Figure 3 shows the danger from the environment due to average precipitation, rainfall erosivity and floods in the three case studies analysed. The maps included identify the areas prone to flooding over a 500-year return period and the maximum height reached by the water (Figure 3a).

The fortified enclosed area of Niebla (Figure 3b) is the one with the highest hazard level. According to the average rainfall, it is an area with low hazard levels (2) and accumulated annual averages of 600–750 mm. The rainfall erosivity presents a very high hazard (5) associated with intensity coefficients >10, which indicate that the daily volume of rainfall is concentrated into a few hours. Despite the fact that the banks of the Tinto River can suffer



(a)



(b)



(c)



(d)

Figure 3.
Water hazards
obtained from model
art-risk 3.0: (a) flood
risk in Andalusia; (b)
water hazards in
Niebla; (c) water
hazards in Marchena;
(d) water hazards in
Almería

floods of up to 2 metres within a 500-year return period, the Niebla fortification is located in an area that is not subject to flooding and more than 10 km from the hazard zones.

The fortified complex of Marchena (Figure 3c) is the site with the lowest hazard levels. The hazard due to average precipitation is low (2), it is an area that is not subject to flooding and the erosive power of the rain is moderate (3).

The fortified complex of Almería (Figure 3d) is in a coastal city, but it is an area that is not subject to flooding and is over 2 km from the port areas that are subject to flooding. The hazard due to average precipitation is very low (1) and has values below 600 mm. The rainfall erosivity

presents a very high hazard (5) associated with intensity coefficients >10 and an irregular distribution of precipitation.

In the three case studies evaluated, the rainfall erosivity is the variable that presents the greatest hazard. This situation corresponds to the characteristics of a Mediterranean macroclimate, in which rainfall is seasonal and highly torrential (Fernanda and López, 2003; Ministerio de Medio Ambiente, y Medio Rural y Marino de España, 2011; Peña Gallardo *et al.*, 2016). Regarding average rainfall, the lowest hazard values recorded in Almería are related to the semi-arid continental Mediterranean microclimate of the area, which is characterised by low, but highly torrential rainfall (Gómez-Zotano *et al.*, 2015). In turn, both Niebla and Marchena have a semi-oceanic Mediterranean microclimate, in which humid airflows from the west and southwest determine the rainfall pattern (Gómez-Zotano *et al.*, 2015) and the values recorded.

3.2 Vulnerability of fortifications according to their state of conservation

To assess the vulnerability of the fortifications, the assessment matrix of the Art-Risk 1 model was used (Ortiz and Ortiz, 2016). Figure 4 shows the results obtained from the vulnerability index in each minimum unit of analysis (towers and walls between towers), indicating the least resilient structures and outlining the areas damaged during the analysed emergencies with a red dashed line. The classification into five groups is based on the natural breaks (Jenk) of the vulnerability indices recorded in all the fortifications analysed. This classification system is based on natural groupings inherent in the data and maximises the differences between classes. 17% is the minimum threshold that separates the group of structures highly vulnerable.

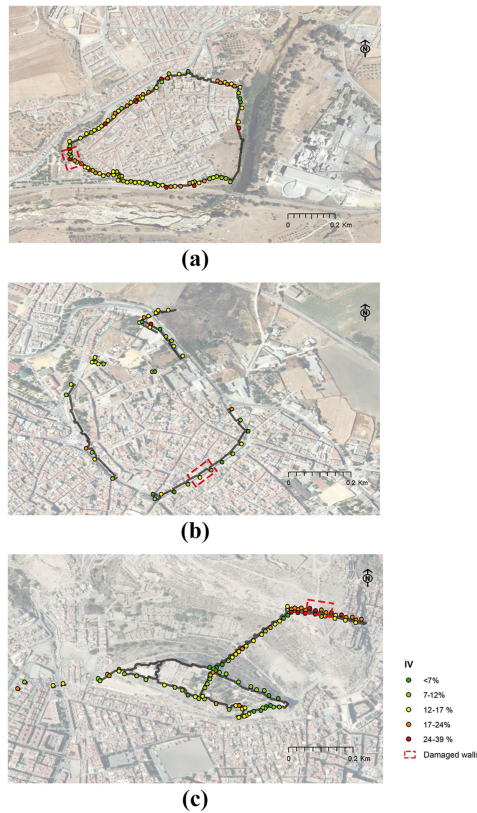
In Niebla, it has been found that 41% of the 106 walls analysed have high vulnerability indices ($>17\%$). These walls are indicated in Figure 4a in orange-red and mainly exhibit detachment (62%) and fractures (58%), weather forms that facilitate the infiltration of water into the interior of the walls and reduce their strength (Figure 5a).

The values recorded in Marchena indicate that 17% of the 40 walls analysed have high vulnerability indices ($>17\%$). The main weather forms are erosion (58%) and fractures (25%) in untreated areas; and moisture stains (50%) and saline concretions (8%) in restored sections. The tower that collapsed after the rainfall in 2017 (Figure 4b) acts as a dividing wall for the modern buildings and, in addition to erosion and fractures, exhibits displacement and loss of material. This tower is currently covered by a protective mesh to prevent new detachments from harming pedestrians (Figure 5b).

In the fortified complex of Almería, 27% of the 94 walls studied have high vulnerability indices ($>17\%$). The monolithic rammed Earth walls are more vulnerable than the stone-lined walls. The most frequent weathering forms are moisture stains (68%), fractures (45%) and detachment (52%) (Figure 5c). The tower affected by the rainfall is made of exposed earthen walls and currently exhibits very high vulnerability.

The cartography formulated in Figure 4 shows that the three collapses occurred in areas in which several of the walls exhibit high vulnerability ($>17\%$). A relationship is also observed between the presence of restorations affected by detachment and fractures, as well as the collapse during rainfall events.

In presence of water, rammed Earth walls behave as a ductile material (Beckett and Thomas, 2011; Jaquin, 2008). During the rains they can suffer displacement, cracking and even collapse, especially in soils with high geotechnical danger that are affected by heavy and prolonged rains (Suradi *et al.*, 2020). In rammed Earth fortifications, the existence of displacements in the lines of the putlog holes can be an indicator of damage associated with the geotechnical problems of the terrain (Jaquin, 2008). These weathering forms, which are studied in the Art-Risk 1 vulnerability matrix model, have not been identified in the field inspections carried out in any of the 3 analysed fortifications. The geotechnical study, the type of foundation and the thickness of the walls showed that the collapses were not associated with this threat.



Note(s): Areas damaged by precipitation events are outlined with a red dashed line

Figure 4. Vulnerability values (VI) at wall level. (a) Niebla; (b) Marchena; (c) Almería

The identified cracks and detachment affect only the restorations mortars and indicate an incorrect grip of the mortars due to the erosion of the original wall. This type of weathering form is associated with different thermal expansion coefficients between the original wall and the additions, as well as increases in the volume of the wall (Jaquin, 2008). Its presence is favourable for the access of water to the interior of the wall, reduces the mechanical resistance and erodes the surface of the original rammed Earth (Beckett *et al.*, 2020). The 3 analysed collapses present this deterioration process.

In a risk study, the proposed method identifies the most problematic points of a wall. The results obtained can be complemented with other characterization and analysis techniques to understand the factors that are causing degradation processes. Thus, in the case of rammed Earth structures, knowing the proportion of lime and clay, granulometry, chemical and mineralogical composition, dry density and construction technique is essential to assess their durability (Jaquin, 2008; Beckett and Thomas, 2011; Ávila *et al.*, 2021; Mota-López *et al.*, 2021; Martín-del-Río *et al.*, 2021). Used as a complement to these studies, the proposed method preserves the geospatial values of vulnerability, allows to identify spatial patterns, and relate them to environment hazards.

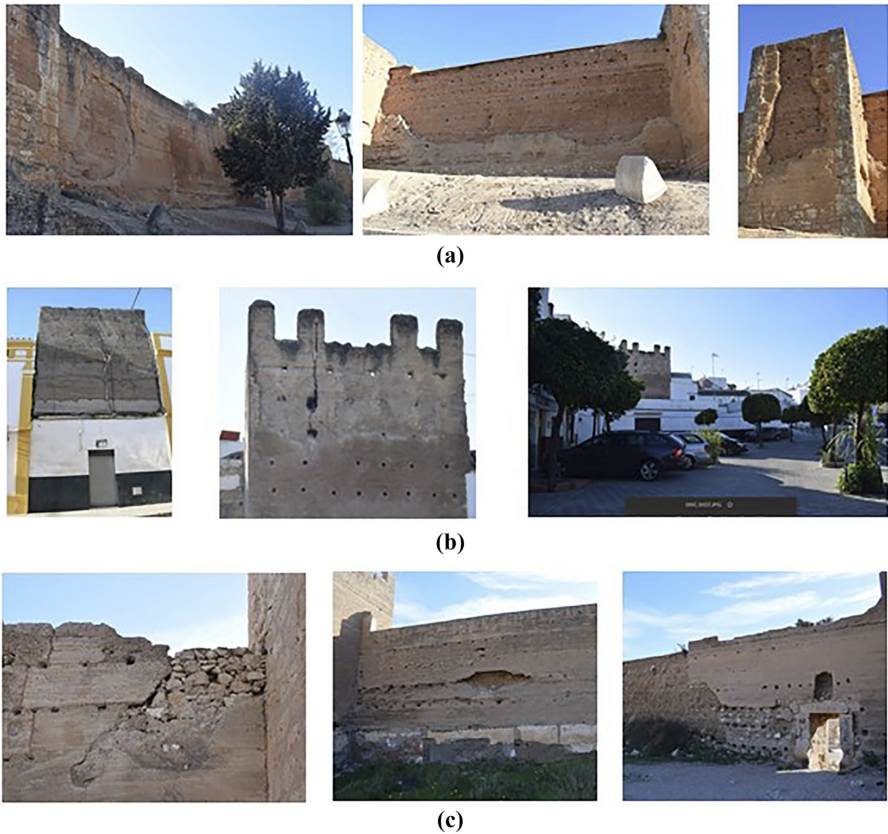


Figure 5. Detachment, fractures and erosion processes identified: (a) Niebla; (b) Marchena; (c) Almería

3.3 Hazards according to the strength, duration and intensity of the rainfalls

3.3.1 *Validation of GPM and GSMaP according to AEMET data.* In order to validate the use of GPM and GSMaP in rainfall monitoring, these satellite resources were compared with the data provided by ground-based AEMET stations. Figure 6 shows a graph with the precipitation data recorded from January to March 2021. The “y” axis values are obtained from the statistical analysis of the series of GPM satellite images (GPM PWM, GPM IR, GPM IMERG) and GSMaP. All the satellite resources tested are capable of detecting the total number of precipitation events that have occurred, although there are large variations between the absolute values of precipitation estimated by the models. In GPM the IR sensors and the IMERG unified algorithm show overestimated values, while the PWM sensors provide very close and slightly underestimated values. GSMaP is the model that provides a better fit to the AEMET data. The data obtained by the GPM PWM sensor also provides a minimum margin of error, but as explained at the beginning of this study, they offer a low temporal resolution.

Figure 7 shows the comparison of data from GSMaP and the AEMET for a full year at points close to the three areas under study. The adjustment level of the model has been obtained from the calculation of the coefficient of determination (r^2). The observed values reach $r^2 = 0.986$ in Morón de la Frontera, $r^2 = 0.961$ in Huelva and $r^2 = 0.857$ in Almería, which indicate that the GSMaP model is a good fit for the weather stations and, despite responding to the values of an area of 11 km², permit the validation of its use in Andalusia.

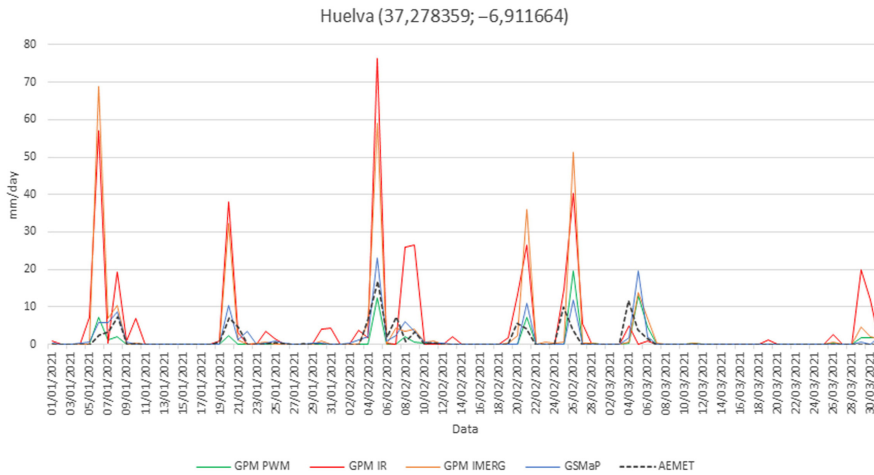


Figure 6. Precipitation data (mm/day) recorded in Huelva from January to march 2021

Note(s): Comparison between ground-based stations (AEMET) and satellite resources (GMP IR, GPM PWM, GPM IMERG, GSMaP)

3.3.2 Use of GSMaP. The presence of water is one of the main dangerous meteorological factors that conditions the durability of the wall (Beckett and Thomas, 2011; Jaquin, 2008; Beckett *et al.*, 2020). Although there are long-term studies that simulate aging processes outdoors (Bui *et al.*, 2009; Richards *et al.*, 2019) and in the laboratory (Cuccurullo *et al.*, 2021; Villacreses *et al.*, 2021), there is a gap regarding the analysis of real cases that makes it difficult to develop realistic risk models.

The maps and graphs obtained from GSMaP enable us to describe the three precipitation events analysed. The maps in Figures 8a, 9a, and 10a indicate the annual accumulated precipitation values in Andalusia. Graphs 8b, 9b and 10b show the daily precipitation values and indicate the distribution and strength of the rainfall. Graphs 8c, 9c and 10c show the hourly precipitation from the days prior to the occurrence of the emergencies and the duration and intensity of the rainfall.

Figure 8 illustrates the Niebla case. In 2019, the accumulated precipitation values ranged between 200 and 300 mm (Figure 8a), ranges lower than those expected according to normal climatic conditions and associated with a dry year. Graph 8B indicates the seasonal nature of the rainfall and places the rainy season from September to May. In general, they are light and moderate rains (3 to 10 mm/day) except for the heavy rains in December that reached 35 mm/day and were responsible for the collapse. Figure 8c shows the hourly distribution of the event and indicates that the rains lasted for several days, but were not very intense. The drizzle began in the early morning of the 16th and remained uninterrupted until 6:00 pm, with maximum peaks of less than 2 mm/hr at noon. It continued to rain on the 18th, 19th and 20th, with maximum peaks of 3.5 mm/hr. The rainfall was accompanied by light north-easterly winds (18-24°) with average speeds below 9 km/hour and wind gusts of less than 20 km/hour (Table 3).

The characteristics of the rainfall that caused the collapse of the Marchena fortification are illustrated in Figure 9. The values of accumulated annual precipitation (300–400 mm) in 2017 were lower than expected according to normal climatic conditions. The rainfall is distributed from October to May, with values between 5 and 25 mm/day and maximums of 31 mm/day in November (Figure 9b). The rainfall associated with the collapse exhibits values of 20 mm/day, being considered moderate-heavy (Alpert *et al.*, 2002). As in the previous case, Figure 9c indicates a rainfall intensity of less than 5 mm/hr, a range far removed from the 15 mm/hr

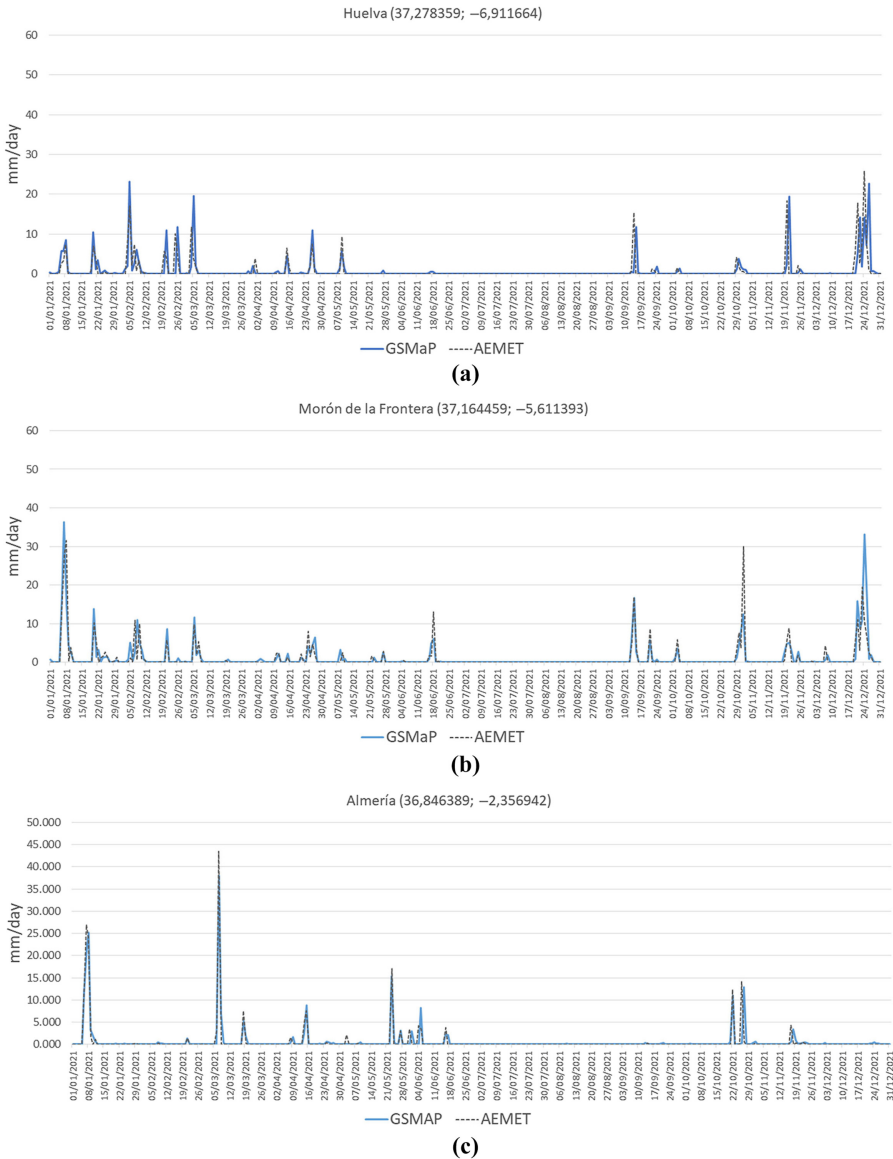
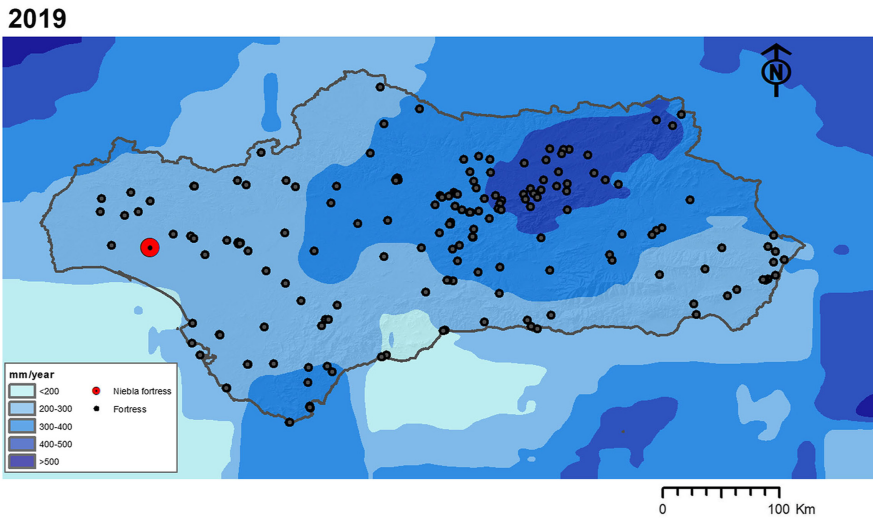


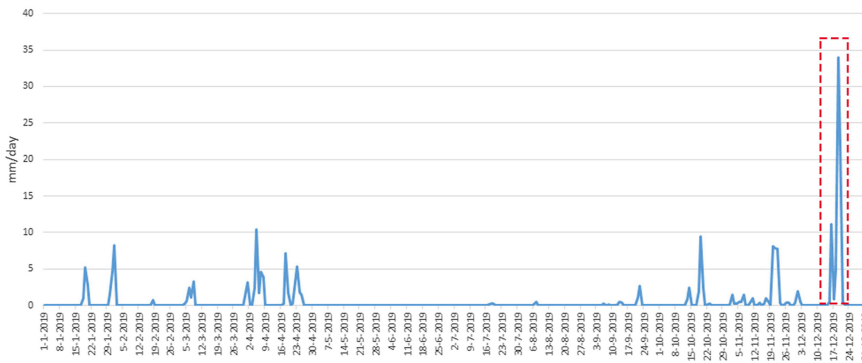
Figure 7. Precipitation data (mm/day) recorded in 2021. Comparison between AEMET ground-based stations and GSMaP reanalysis. (a) Huelva; (b) Morón de la Frontera and (c) Almería

considered to be a risk by the AEMET. The average wind speeds below 3.3 km/hour indicate calm winds on those days with slight temporary increases in the form of gusts of less than 10 km/hour (Table 3).

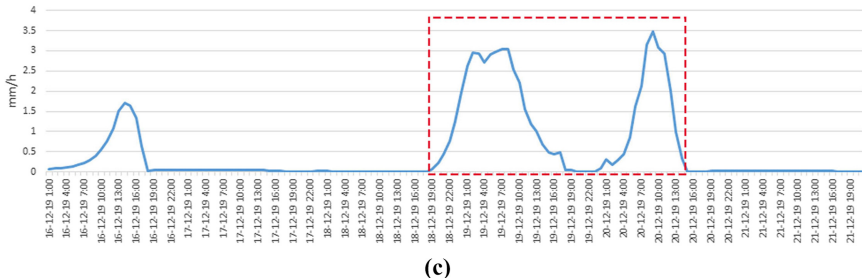
In turn, Figure 10 outlines the emergency experienced at the fortification of Almería. The accumulated annual precipitation values in 2021 ranged between 200 and 300 mm, values higher than those expected in terms of normal climatic conditions. The rainfall between October and May with maximums of 32 mm/day in March and periods without rainfall in



(a)



(b)



(c)

Figure 8. Rainfall that caused the collapse in Niebla (december 2019). (a) accumulated rainfall in 2019 in Andalusia; (b) Sstrength of the rainfall in mm/day; (c) intensity of the rainfall in mm/hour during the day of the collapse

Note(s): The dates on which the collapse occurred are outlined with a red dashed line

summer and winter. The damage detected in the wall was caused by the light-moderate rains in November that reached maximums of 11 mm/day (Figure 10b). Figure 10c shows that it is rainfall of weak intensity with maximums of 2 mm/hr, but that it continuously increases

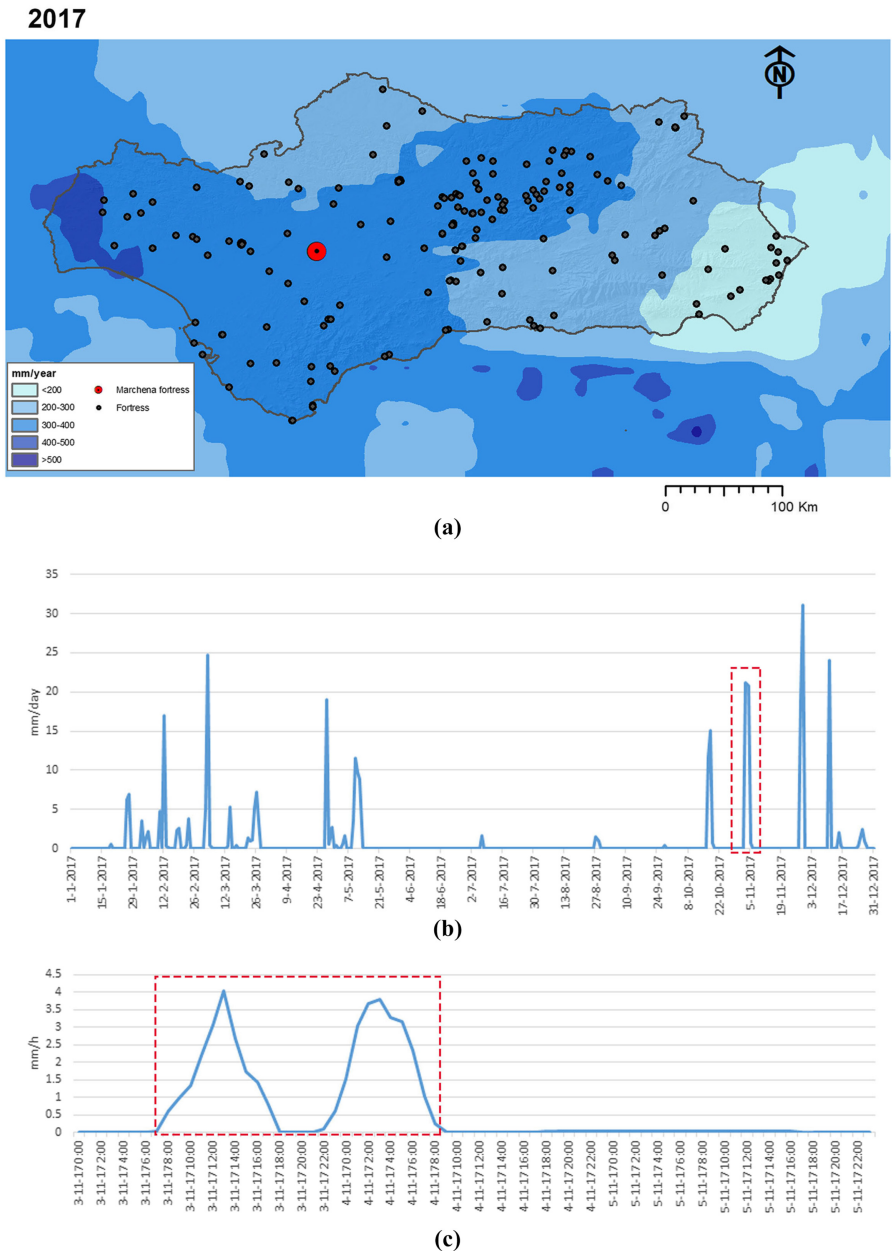
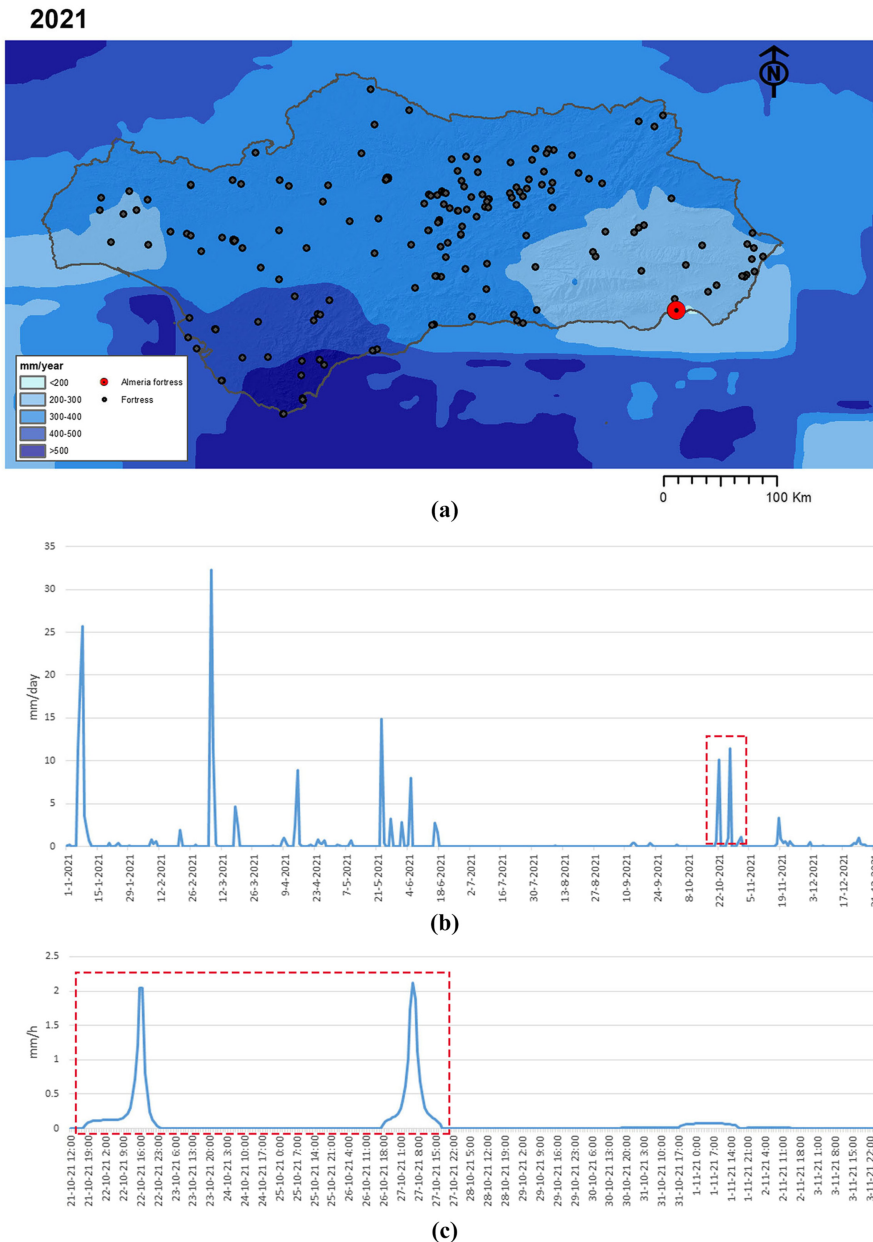


Figure 9. Rainfall that caused the collapse in Marchena (november 2017). (a) Accumulated rainfall in 2017 in Andalusia; (b) Strength of the rainfall in mm/day; (c) Intensity of the rainfall in mm/hour during the collapse

Note(s): The dates on which the collapse occurred are outlined with a red dashed line

during the 22nd and 27th of November. The prevailing winds were from the north, northeast and east. They were light winds with average speeds below 10 km/hour and gusts of wind below 20 km/hour (Table 3).



Note(s): The dates on which the collapse occurred are outlined with a red dashed line

Figure 10. Rainfall that caused the collapse in Almería (october 2021). (a) accumulated rainfall in 2021 in Andalusia; (b) strength of the rainfall in mm/day; (c) intensity of the rainfall in mm/hour during the collapse

The results obtained indicate that there were no serious episodes of torrential rainfall or strong winds that could be the cause of the collapses in the fortifications analysed. The winds recorded are always light and the intensity of the rainfall is weak. Thus, the daily volume of

Table 3.

Strength and direction of the winds during the rainfall that caused the collapses (prepared from AEMET data)

	Date	Average speed (km/h)	Gust (km/h)	Direction (°)
Niebla	16/12/2019	6.9	17.2	21
	17/12/2019	3.3	10	30
	18/12/2019	4.2	11.7	18
	19/12/2019	8.6	16.9	20
	20/12/2019	7.5	18.1	24
	21/12/2019	7.2	16.4	24
Marchena	03/11/2017	1.4	7.2	22
	04/11/2017	3.3	10	23
	05/11/2017	0.8	3.6	26
Almería	21/11/2021	6.1	11.7	25
	22/11/2021	6.7	14.4	25
	23/11/2021	7.5	16.4	23
	24/11/2021	3.3	12.8	34
	25/11/2021	4.2	14.4	26
	26/11/2021	5.3	11.7	99
	27/11/2021	6.7	20	99

falling water and the long duration in time seem to be the probable causes that make the rainfall moderate-heavy and hazardous for this type of construction in the rammed Earth fortifications analysed. In other words, the time factor seems to condition the hazard from the rainfall.

4. Concluding discussion

The study conducted presents a work methodology based on the use of vulnerability indices, geographic information systems and satellite resources capable of recording the hazards and vulnerability associated with a risk situation due to rainfall in rammed Earth fortifications. This model has been validated and tested in three past situations in which rainfall caused the collapse of historic rammed Earth fortifications in Andalusia.

The data obtained from satellite images are consistent data that allows to compare emergencies that occurred in different places and dates. The validation of the two main satellites available allows to knowing their precision-accuracy and reduces the uncertainty associated with the incorporation in the risk model. The analysis of satellite resources indicates that GSMaP offers a better fit to data from ground-based weather stations and, at least in the cases analysed, provides greater precision in areas far from the coast. The high coefficients of determination observed (>0.85) support its selection in the monitoring of rainfall events in Andalusia. Although GPM IMERG is capable of accurately identifying the occurrence of rainfall, it overestimates the absolute values.

In the cases analysed, the three emergencies occurred in environments with a moderate-high hazard level in terms of the erosive power and intensity of the rainfall and a low hazard level in terms of the average accumulated rainfall. Despite this, the rainfall that generated the emergencies did not exceed 5 mm/hr and cannot be considered intense rainfall according to the [AEMET \(2015\)](#). The long duration of the rainfall, which ranged between 2 and 5 consecutive days, seems to be the cause of the weakening of the earthen walls and the damage that occurred to areas in a worse state of conservation, and which are more vulnerable to water infiltration. In this vein, previous studies have already pointed out, both in the theory ([Beckett et al., 2020](#)) and in simulated tests ([Cuccurullo et al., 2021](#); [Richards et al., 2019](#)), the hazard associated with long-term rainfalls that favour the internal dampening and mechanical weakening of the earthen wall structures. The results obtained in this study

corroborate these hypotheses and future studies should carry out *in situ* monitoring to compare the data recorded by satellite and laboratory tests to better understand the factors involved in the collapse of rammed Earth fortifications caused by rainfall.

As expected, the areas with the most vulnerable walls and towers are those that suffered collapses during the rainfall. In turn, the correlation observed between the presence of restorations that tend to fracture, become dislodged and separate from the original and the occurrence of collapses is also a critical factor. It seems possible that the differences in the swelling and drying processes associated with a rainfall event, and the loss of the mechanical and adhesive capacities of the original mortar when moistened (Morel *et al.*, 2012) are the direct cause of the collapses of restoration mortars. Currently, the poor performance of mortars with lime and cement additives in historical rammed Earth walls has been pointed out by various authors (Gomes *et al.*, 2016, 2018; Silva *et al.*, 2018), but there are still numerous factors to evaluate regarding the degree of functionality and durability presented by restoration mortars in different rainfall hazard contexts.

In summary, the preliminary results of this study help to identify the most problematic points of a wall and evaluate the duration, strength, and intensity of the rainfall during an emergency. Characterization studies and laboratory techniques must be added to this methodology in order to understand the degradation processes of historical rammed Earth walls triggered by rainfall. The results are of great interest for the development of more realistic risk models, capable of forecasting emergency situations in the future.

References

- ABCandalucía (2020), “Caen partes de la milenaria muralla de Niebla a causa del temporal de lluvia y viento”, *ABCandalucía*, 21 de diciembre de 2019, available at: https://sevilla.abc.es/andalucia/huelva/sevi-huelva-caen-partes-milenaria-muralla-niebla-causa-temporal-lluvia-y-viento-201912212338_noticia.html#disqus_thread (accessed 06 February 2022).
- ABCdesevilla (2017), “Se desprende parte de la muralla almohade de Marchena a causa de la lluvia y un rayo”, *ABCdesevilla*, 3 de noviembre de 2017, available at: https://sevilla.abc.es/provincia/sevi-desprende-parte-muralla-almohade-marchena-causa-lluvia-y-rayo-201711032330_noticia.html?ref=https%3A%2F%2Fwww.google.com%2F (accessed 06 February 2022).
- AEMET: Meteorology Statal Agency of Spain (2015), “Manual de uso de términos meteorológicos”, available at: http://www.aemet.es/documentos/es/eltiempo/prediccion/comun/Manual_de_uso_de_terminos_met_2015.pdf.
- Alpert, P., Ben-Gai, T., Baharad, A., Benjamini, Y., Yekutieli, D., Colacino, M., Diodato, L., Ramis, C., Homar, V., Romero, R., Michaelides, S. and Manes, A. (2002), “The paradoxical increase of Mediterranean extreme daily rainfall in spite of decrease in total values”, *Geophysical Research Letters*, Vol. 29 No. 11, pp. 3131-3134, doi: 10.1029/2001GL013554.
- Ávila, F., Puertas, E. and Gallego, R. (2021), “Characterization of the mechanical and physical properties of unstabilized rammed earth: a review”, *Construction and Building Materials*, Vol. 270, 121435, doi: 10.1016/J.CONBUILDMAT.2020.121435.
- Beckett, C. and Thomas, S. (2011), “The role of material structure in compacted earthen building materials: implications for design and construction”, Doctoral dissertation, Durham University.
- Beckett, C.T.S., Jaquin, P.A. and Morel, J.C. (2020), “Weathering the storm: a framework to assess the resistance of earthen structures to water damage”, *Construction and Building Materials*, Vol. 242, 118098, doi: 10.1016/J.CONBUILDMAT.2020.118098.
- Bolvin, D.T., Braithwaite, D., Hsu, K., Joyce, R., Kidd, C., Nelkin, E.J., Xie, P., Huffman, G., Bolvin, D.T., Braithwaite, D., Hsu, K., Joyce, R., Kidd, C., Nelkin, E.J. and Xie, P. (2015), “NASA global precipitation measurement (GPM) integrated multi-satellitE retrievals for GPM (IMERG) prepared for: global precipitation measurement (GPM) national Aeronautics and space

- administration (NASA)", *Algorithm Theoretical Basis Document (ATBD) Version 4.5*, 26 November, available at: https://pmm.nasa.gov/sites/default/files/imce/times_allsat.jpg.
- Bonazza, A., Sardella, A., Kaiser, A., Cacciotti, R., De Nuntii, P., Hanus, C., Maxwell, I., Drdáký, T. and Drdáký, M. (2021), "Safeguarding cultural heritage from climate change related hydrometeorological hazards in Central Europe", *International Journal of Disaster Risk Reduction*, Vol. 63, 102455, doi: [10.1016/J.IJDRR.2021.102455](https://doi.org/10.1016/J.IJDRR.2021.102455).
- Cacciotti, R., Kaiser, A., Sardella, A., De Nuntii, P., Drdáký, M., Hanus, C. and Bonazza, A. (2021), "Climate change-induced disasters and cultural heritage: optimizing management strategies in Central Europe", *Climate Risk Management*, Vol. 32, 100301, doi: [10.1016/J.CRM.2021.100301](https://doi.org/10.1016/J.CRM.2021.100301).
- Cagigas-Muñiz, D., Martín, J., Rieto, A., Romero, A., Ortiz, R., Macías-Bernal, J. and Ortiz, P. (2018), "A new tool based on Artificial Intelligence and GIS for preventive conservation of heritage buildings", *International Conference Resilience and Sustainable of Cities in Hazardous Environments*, available at: <https://idus.us.es/handle/11441/98875>.
- Cagigas-Muñiz, D., Ortiz, R., Ortiz, P., Prieto, A., Vizuete, M.A., Becerra, J., Segura, D. and Chavez, M.A. (2020), "Registro software: art-Risk 3.0. Software basado en Inteligencia Artificial aplicada a la conservación preventiva de PH (iglesias)", SE-967-19, UPO, US e IVCR+i, available at: <https://www.upo.es/investiga/art-risk-service/art-risk3/index.html>.
- Canivell, J. and González Serrano, A.M. (2013), "Fábricas de tapia en la ciudad histórica de Niebla", in *G. Viñuales Arquitectura Vernácula Iberoamericana*, Red AVI, Sevilla.
- Canivell, J., Rodríguez García, R., González Serrano, A.M. and Romero Girón, A. (2020), "Assessment of heritage rammed-earth buildings. The Alcázar of King Don Pedro I (Spain)", ASCE.
- Cuccurullo, A., Gallipoli, D., Bruno, A.W., Augarde, C., Hughes, P. and La Borderie, C. (2021), "A comparative study of the effects of particle grading and compaction effort on the strength and stiffness of earth building materials at different humidity levels", *Construction and Building Materials*, Vol. 306, 124770, doi: [10.1016/J.CONBUILDMAT.2021.124770](https://doi.org/10.1016/J.CONBUILDMAT.2021.124770).
- Diario de Almería (2021), "La muralla de la Alcazaba se agujerea a un ritmo vergonzoso", *Diario de Almería*, 5 de noviembre de 2021, available at: https://www.diariodealmeria.es/almeria/muralla-Alcazaba-agujerea-ritmo-vergonzoso_0_1626138862.html (accessed 06 February 2022).
- Drdáký, M. and Cacciotti, R. (2020), "Cultural heritage resilience: manual for owners and managers", (ProteCHt2save. Interreg Central Europe (ed.)), available at: http://www.itam.cas.cz/miranda2/export/sitesavcr/utam/sys/galerie-download/ProteCHt2save/ManualEN_03.07.2020_RGB_final.pdf.
- Fernanda, M. and López, P. (2003), "El clima de Andalucía", in López Ontiveros, A. (Ed.), *Geografía de Andalucía*, pp. 137-174.
- Ferreira, T.M. and Santos, P.P. (2020), "An integrated approach for assessing flood risk in historic city centres", *Water (Switzerland)*, Vol. 12 No. 6, doi: [10.3390/w12061648](https://doi.org/10.3390/w12061648).
- Figueiredo, R., Romão, X. and Paupério, E. (2021), "Component-based flood vulnerability modelling for cultural heritage buildings", *International Journal of Disaster Risk Reduction*, Vol. 61, 102323, doi: [10.1016/J.IJDRR.2021.102323](https://doi.org/10.1016/J.IJDRR.2021.102323).
- Gómez-Zotano, J., Alcántara-Manzanares, J., Olmedo-Cobo, J. and Martínez-Ibarra, E. (2015), "La sistematización del clima mediterráneo: identificación, clasificación y caracterización climática de Andalucía (España)", *Revista de Geografía Norte Grande*, Vol. 61, pp. 161-180, available at: https://scielo.conicyt.cl/scielo.php?pid=S0718-34022015000200009&script=sci_arttext.
- Gomes, M.I., Gonçalves, T.D. and Faria, P. (2016), "Hydric behavior of Earth materials and the effects of their stabilization with cement or lime: study on repair mortars for historical rammed Earth structures", *Journal of Materials in Civil Engineering*, Vol. 28 No. 7, 04016041, doi: [10.1061/\(ASCE\)MT.1943-5533.0001536](https://doi.org/10.1061/(ASCE)MT.1943-5533.0001536).
- Gomes, M.I., Faria, P. and Gonçalves, T.D. (2018), "Earth-based mortars for repair and protection of rammed earth walls. Stabilization with mineral binders and fibers", *Journal of Cleaner Production*, Vol. 172, pp. 2401-2414, doi: [10.1016/J.JCLEPRO.2017.11.170](https://doi.org/10.1016/J.JCLEPRO.2017.11.170).

- Gutiérrez-Carrillo, M.L., Bestué Cardiel, I., Molero Melgarejo, E. and Marcos Cobaleda, M. (2020), "Pathologic and risk analysis of the Lojuela Castle (Granada-Spain): methodology and preventive conservation for medieval earthen fortifications", *Applied Sciences*, Vol. 10 No. 18, p. 6491.
- Hosseinzadehtalaei, P., Tabari, H. and Willems, P. (2020), "Climate change impact on short-duration extreme precipitation and intensity–duration–frequency curves over Europe", *Journal of Hydrology*, Vol. 590, 125249, doi: [10.1016/j.jhydrol.2020.125249](https://doi.org/10.1016/j.jhydrol.2020.125249).
- Huffman, G.J., Bolvin, D.T., Braithwaite, D., Hsu, K.L., Joyce, R.J., Kidd, C., Nelkin, E.J., Sorooshian, S., Stocker, E.F., Tan, J., Wolff, D.B. and Xie, P. (2020), "Integrated multi-satellite retrievals for the global precipitation measurement (GPM) mission (IMERG)", *Advances in Global Change Research*, Vol. 67, pp. 343-353, doi: [10.1007/978-3-030-24568-9_19](https://doi.org/10.1007/978-3-030-24568-9_19).
- Jaquin, P.A. (2008), "Analysis of historic rammed Earth construction", Doctoral dissertation, Durham University.
- Kharin, V.V., Zwiers, F.W., Zhang, X. and Wehner, M. (2013), "Changes in temperature and precipitation extremes in the CMIP5 ensemble", *Climatic Change*, Vol. 119 No. 2, pp. 345-357, doi: [10.1007/S10584-013-0705-8/FIGURES/6](https://doi.org/10.1007/S10584-013-0705-8/FIGURES/6).
- Liang, S. (2017), "Comprehensive remote sensing", *Comprehensive Remote Sensing*, Vol. 1 No. 9, doi: [10.1016/c2014-1-03229-2](https://doi.org/10.1016/c2014-1-03229-2).
- Martín-del-Río, J.J., Canivell, J., Torres-González, M., Mascort-Albea, E.J., Romero-Hernández, R., Alducin-Ochoa, J.M. and Alejandro-Sánchez, F.J. (2021), "Analysis of the materials and state of conservation of the medieval rammed earth walls of Seville (Spain)", *Journal of Building Engineering*, Vol. 44, 103381.
- Mega, T., Ushio, T., Matsuda, T., Kubota, T., Kachi, M. and Oki, R. (2019), "Gauge-adjusted global satellite mapping of precipitation", *IEEE Transactions on Geoscience and Remote Sensing*, Vol. 57 No. 4, pp. 1928-1935, doi: [10.1109/TGRS.2018.2870199](https://doi.org/10.1109/TGRS.2018.2870199).
- Ministerio de Medio Ambiente, y Medio Rural y Marino de España (2011), *Berian Climate Atlas: air Temperature and precipitation (1971-2000)*, Madrid.
- Morel, J.C., Bui, Q.B. and Hamard, E. (2012), "Weathering and durability of earthen material and structures", in *Modern Earth Buildings: Materials, Engineering, Constructions and Applications*, Woodhead Publishing, pp. 282-303, doi: [10.1533/9780857096166.2.282](https://doi.org/10.1533/9780857096166.2.282).
- Moreno, M., Ortiz, P. and Ortiz, R. (2019), "Vulnerability study of earth walls in urban fortifications using cause-effect matrixes and gis: the case of seville, carmona and estepa defensive fences", *Mediterranean Archaeology and Archaeometry*, Vol. 19 No. 3, pp. 119-138, doi: [10.5281/zenodo.3583063](https://doi.org/10.5281/zenodo.3583063).
- Moreno, M., Ortiz, R. and Ortiz, P. (2021), "Incendios en paisajes patrimoniales naturales: análisis y evaluación de riesgos en fortificaciones mediante el uso del Global Wildfire Information System", *Revista PH*, Iaph, pp. 413-419, doi: [10.33349/2021.104.4976](https://doi.org/10.33349/2021.104.4976).
- Moreno, M., Prieto, A.J., Ortiz, R., Cagigas-Muñiz, D., Becerra, J., Garrido-Vizueté, M.A., Segura, D., Macías-Bernal, J.M., Chávez, M.J. and Ortiz, P. (2022a), "Preventive conservation and restoration monitoring of heritage buildings based on fuzzy logic", *International Journal of Architectural Heritage*, Vol. 16, pp. 1-18.
- Moreno, M., Prieto, A.J., Ortiz, R., Cagigas-Muñiz, D., Becerra, J., Garrido-Vizueté, M.A., Segura, D., Macías-Bernal, J.M., Chávez, M.J. and Ortiz, P. (2022b), "ART-RISK 3.0 a fuzzy—based platform that combine GIS and expert assessments for conservation strategies in cultural heritage", *Journal of Cultural Heritage*, Vol. 55, pp. 263-276.
- Moreno, M., Bertolín, C., Ortiz, P. and Ortiz, R. (2022c), "Satellite product to map drought and extreme precipitation trend in Andalusia, Spain: a novel method to assess heritage landscapes at risk", *International Journal of Applied Earth Observation and Geoinformation*, No. 110, p. 102810.
- Mota-Lopez, M.L., Maderuelo-Sanz, R., Pastor-Valle, J.D., Meneses-Rodríguez, J.M. and Romero-Casado, A. (2021), "Analytical characterization of the almohad rammed-earth wall of Cáceres, Spain", *Construction and Building Materials*, Vol. 273, 121676.

- Luo, Y., Yin, B., Peng, X., Xu, Y. and Zhang, L. (2019), "Wind-rain erosion of Fujian Tulou Hakka earth buildings", *Sustainable Cities and Society*, Vol. 50, 101666.
- Okamoto, K., Ushio, T., Iguchi, T., Takahashi, N. and Iwanami, K. (2005), "The global satellite mapping of precipitation (GSMaP) project", *International Geoscience and Remote Sensing Symposium (IGARSS)*, Vol. 5, pp. 3414-3416, doi: [10.1109/IGARSS.2005.1526575](https://doi.org/10.1109/IGARSS.2005.1526575).
- Organización Meteorológica Mundial (2012), "Índice normalizado de precipitación - guía del usuario", Ginebra.
- Ortiz, Rocío and Ortiz, P. (2016), "Vulnerability index: a new approach for preventive conservation of monuments", *International Journal of Architectural Heritage*, Vol. 10 No. 8, pp. 1078-1100, doi: [10.1080/15583058.2016.1186758](https://doi.org/10.1080/15583058.2016.1186758).
- Ortiz Calderón, R., Moreno Falcón, M., Becerra Luna, J., Corona Corrales, S. and Ortiz Calderón, P. (2021), "El análisis de riesgos en los centros históricos: estudio de las fortificaciones urbanas del centro histórico de Sevilla", *Revista PH*, October, p. 342, doi: [10.33349/2021.104.4942](https://doi.org/10.33349/2021.104.4942).
- Ortiz, R., Garrido-Vizuet, M., Prieto, A., Macías-Bernal, J., Becerra, J., Benítez, J., Gómez-Morón, M., Martín, J., Segura, D., Tirado-Hernández, A., Turbay, I., Chávez, M., Cagigas-Muñiz, D., Vázquez-González, A., Contreras-Zamorano, G., Cisternas, V. and Ortiz, P. (2018), "Preventive conservation of monuments based on DELPHI method and fuzzy Logic", *International conference resilience and sustainable of cities in hazardous environments*".
- Ortiz, P., Macias, J.M., Ortiz, R., Prieto, A., Vizuet, A., Cagigas, D., Martín, J.M., Becerra, J., Turbay, I., Gómez, A., Vázquez, A., Segura, D., Chávez, J., Benítez, J., Tirado, A., Contreras, G., Cisternas, V., Rodríguez, B., Abreu, D., Cepero, A. and Díaz, A. (2019), "Manual de usuario: software ART-RISK 3.0", available at: https://www.upo.es/investiga/art-risk-service/art-risk3/files/Manual_Usuario_Espa%C3%B1ol_ART-RISK_3.0.pdf.
- Peña Gallardo, M., Gámiz Fortis, S.R., Castro Díez, A.Y. and Esteban-Parra, M.J. (2016), "Análisis comparativo de índices de sequía en Andalucía para el periodo 1901-2012", *Cuadernos de Investigación Geográfica/Geographical Research Letters*, Vol. 42 No. 42, pp. 67-88, ISSN 0211-6820, ISSN-e 1697-9540, doi: [10.18172/cig.2946](https://doi.org/10.18172/cig.2946).
- Prieto, A.J., Turbay, I., Ortiz, R., Chávez, M.J., Macías-Bernal, J.M. and Ortiz, P. (2020), "A fuzzy logic approach to preventive conservation of cultural heritage churches in Popayán, Colombia", *International Journal of Architectural Heritage*, pp. 1-20, doi: [10.1080/15583058.2020.1737892](https://doi.org/10.1080/15583058.2020.1737892).
- Richards, J., Zhao, G., Zhang, H. and Viles, H. (2019), "A controlled field experiment to investigate the deterioration of earthen heritage by wind and rain", *Heritage Science*, Vol. 7 No. 1, pp. 1-13, doi: [10.1186/S40494-019-0293-7/FIGURES/6](https://doi.org/10.1186/S40494-019-0293-7/FIGURES/6).
- Sabbioni, C., Brimblecombe, P. and Cassar, M. (2010), "THE atlas of climate change impact on EUROPEAN cultural heritage scientific analysis and management strategies NOAH'S ark global climate change impact on built heritage and cultural landscapes", available at: www.anthempress.com.
- Schauwecker, S., Gascón, E., Park, S., Ruiz-Villanueva, V., Schwarb, M., Sempere-Torres, D., Stoffel, M., Vitolo, C. and Rohrer, M. (2019), "Anticipating cascading effects of extreme precipitation with pathway schemes - three case studies from Europe", *Environment International*, Vol. 127, pp. 291-304, doi: [10.1016/J.ENVINT.2019.02.072](https://doi.org/10.1016/J.ENVINT.2019.02.072).
- Sesana, E., Gagnon, A.S., Bonazza, A. and Hughes, J.J. (2020), "An integrated approach for assessing the vulnerability of World Heritage Sites to climate change impacts", *Journal of Cultural Heritage*, Vol. 41, pp. 211-224, doi: [10.1016/j.culher.2019.06.013](https://doi.org/10.1016/j.culher.2019.06.013).
- Silva, R.A., Domínguez-Martínez, O., Oliveira, D.V. and Pereira, E.B. (2018), "Comparison of the performance of hydraulic lime- and clay-based grouts in the repair of rammed earth", *Construction and Building Materials*, Vol. 193, pp. 384-394, doi: [10.1016/j.conbuildmat.2018.10.207](https://doi.org/10.1016/j.conbuildmat.2018.10.207).
- Smith, G. (2018), *Geospatial Analysis: A Comprehensive Guide*, 6th ed., available at: <https://www.spatialanalysisonline.com/HTML/index.html>.

-
- Su, N., Yang, B., Chen, W., Xu, L. and Li, Y. (2022), "Influence of prevailing wind direction on sapping quantity of rammed Earth great wall of the ming dynasty", *Coatings*, Vol. 12 No. 5, p. 707.
- Sun, Q., Miao, C., Duan, Q., Ashouri, H., Sorooshian, S. and Hsu, K.-L. (2018), "A review of global precipitation data sets: data sources, estimation, and intercomparisons", *Reviews of Geophysics*, Vol. 56 No. 1, pp. 79-107, doi: [10.1002/2017RG000574](https://doi.org/10.1002/2017RG000574).
- Suradi, M., Fourie, A., Beckett, C. and Buzzi, O. (2020), "Rainfall-induced landslides: development of a simple screening tool based on rainfall data and unsaturated soil mechanics principles", *Unsaturated Soils: Research and Applications*, CRC Press, pp. 1459-1465.
- Tabari, H. (2020), "Climate change impact on flood and extreme precipitation increases with water availability", *Scientific Reports*, Vol. 10 No. 1, pp. 1-10, doi: [10.1038/s41598-020-70816-2](https://doi.org/10.1038/s41598-020-70816-2).
- Trenberth, K.E. (2011), "Changes in precipitation with climate change", *Climate Research*, Vol. 47 Nos 1-2, pp. 123-138, doi: [10.3354/CR00953](https://doi.org/10.3354/CR00953).
- Valor Piechotta, M. (2004), "Algunos ejemplos de construcciones defensivas almohades en la provincia de Sevilla", *Los Almohades. Su patrimonio arquitectónico y arqueológico en el sur de al-Andalus*, Junta de Andalucía, Sevilla, pp. 145-163.
- Villacreses, J.P., Granados, J., Caicedo, B., Torres-Rodas, P. and Yépez, F. (2021), "Seismic and hydromechanical performance of rammed earth walls under changing environmental conditions", *Construction and Building Materials*, Vol. 300, 124331.

Corresponding author

Mónica Moreno can be contacted at: mmorfal@upo.es